Adaptive Fuzzy Lyapunov-based Model Predictive Control for Parallel Platform Driving Simulators

Transactions of the Institute of Measurement and Control
XX(X):1–26

DOI: 10.1177/ToBeAssigned
www.sagepub.com/
SAGE

Cuong Nguyen Manh[1], Nhu Toan Nguyen[1], Nam Bui Duy[2] and Tung Lam Nguyen[1]

Abstract

The paper proposes an adaptive Lyapunov-based nonlinear model predictive control to cope with the problems in nonlinear systems subjecting to system constraints and unknown disturbances of the parallel car driving simulator. Commonly, standard nonlinear controllers could guarantee the overall system stability for the parallel structure. However, the constraints tend to impact the control performance and stability adversely. Therefore, model predictive control (MPC) plays a vital role in the proposed technique to explicitly consider all the practical constraints and simultaneously enhance the system's robustness. Nevertheless, the accuracy of the modeling process has a significant effect on the MPC performance, and thus, the convergence cannot be guaranteed in the presence of the model uncertainties. To overcome this problem, by the merit of the fuzzy adaptive law, the control system takes the disturbances and unmodelled parameters into account. Moreover, the feasibility and stability of the approach, which is the fundamental problem of MPC, are ensured according to the Lyapunov-based nonlinear controller, Backstepping aggregated with Sliding Mode Control (SMC), and hence inherit advantages of these controls. Simulation results show the efficiency and superior constituted controllers of the proposed method.

Keywords

Nonlinear Model Predictive Control (NMPC), Fuzzy logic, Adaptive control, Car Driving Simulator (CDS)

[1]Hanoi University of Science and Technology, Hanoi, Vietnam
[2]VNU University of Engineering and Technology, Hanoi, Vietnam

Corresponding author:
Tung Nguyen Lam, Hanoi University of Science and Technology, Hanoi, Vietnam
Email: lam.nguyentung@hust.edu.vn

Prepared using sagej.cls *[Version: 2017/01/17 v1.20]*

Introduction

Parallel robots have been increasingly prevalent in many fields, including industry, military, and medical applications. There are many types of parallel structures have been proposed such as three degree of freedom (3 DOF) Quan et al. (2020), Khalifa et al. (2018), Dindorf and Wos (2019), or six degree of freedom (6 DOF) Campa et al. (2016), Rastegarpanah et al. (2016) which are widely applied especially in rehabilitation. Besides, several potential applications of parallel robots are taken into account, for instance, high-speed manipulation, material handling, planetary explorers, and pointing devices in terrestrial and space environments. Moreover, for the motion simulation scope, parallel robots can accurately simulate the actual motions of flight, car driving simulation, and marine motion in particular scenarios. In addition, the driving simulation model effectively reduces risks induced by methods based on actual vehicles and minimizes the driver's unexpected effects at the first period of training progress. Compared with serial robots, which are compromised between precision, complexity, mass, and cost, the parallel robot provides higher accuracy and dynamic performance. In detail, they can achieve high rigidity with a smaller mass of manipulators, that provide better accuracy and necessary speed in motion and promote the application of parallel driving simulation platforms. Commonly, most of these models require highly certain stiffness because the external load is shared by multiple legs, as well as high acceleration and speed due to the low inertia of the moving structure Jin et al. (2015).

Comprehensive research on the kinematic and dynamic model of the system is of paramount importance to designing an effective controller. For the parallel robot 6 DOF, its forward and reverse kinematics models are studied explicitly in Thomas et al. (2022) and Campa et al. (2016). The noticeable advantage of the 6 DOF parallel robot is the ability to maneuver flexibly with high precision. However, the motion complexity due to the combination of the six actuators causes many challenges for control designs, especially in disturbances and time delay. Therefore, in order to attenuate the model complexity as well as computational time, the configurations with fewer joints and DOF Gouttefarde et al. (2015), and Quan et al. (2020) are considered as the more appropriate measures for practical applications. In addition, the impact of delay transmission and redundancy of actuators are also reduced in lower DOF cases. Thus, based on related research works and the application of our parallel robot in the car driving problem, a four-DOF platform (4 DOFP) is constructed, which includes four motions: rotational motions around OX, OY, and OZ axes, and translation motion along the OZ axis.

In general, the control design for the trajectory tracking problem of the parallel robot system is an attractive field with many challenging issues due to its diversity of system configuration and highly nonlinear characteristics. Linear control methods such as proportional-integral-derivative (PID) and linear-quadratic-regulator (LQR) are widely used because of their ease of implementation in practice. However, the cancellation of some useful nonlinear information of the system could reduce the accuracy and lead to divergence in some cases. Combining linear controllers with an adaptive scheme is one of the effective approaches to improve the tracking performance Salas et al. (2019) and Jamshidifar et al. (2015). In Tian (2021), a time-delay compensation method based on PI-based dynamic matrix control for the networked control system is proposed. The novel objective function of dynamic matrix control is integrated with the PI feedback structure to obtain the optimal control increment value, leading to the noticeable reduction of the impact of mismatch and interference on the system. In Choubey and Ohri (2022), the linear quadratic regulator and proportional integral derivative controller are proposed for trajectory tracking problem of 3-DOF Maryland manipulator, in which the control parameters are tuned by gray wolf optimizer (GWO) algorithm. On the other hand, nonlinear control techniques are typically

employed for nonlinear systems such as parallel robots to design trajectory tracking controllers. One of the most prevalent nonlinear control methods is the Backstepping technique and its variations Thi et al. (2019), Truong et al. (2021), and Yu et al. (2018), which is based on the recursive design procedure where the derivation of the Lyapunov function is linked with the design of feedback control signals. However, the control quality is degraded if the system's parametric uncertainties and noise components exist, leading to the explosion of terms' phenomena. Another commonplace nonlinear feedback control method is sliding mode control (SMC) Oumer and Hunde (2015), Hoang and Vuong (2018), and Lv et al. (2017) because of its advantageous features, including fast dynamic response and robustness to external disturbances and uncertain parameters. Nevertheless, the chattering phenomenon generated by the SMC controller is always a concerning problem that potentially damages the control performance, especially in the hardware system. Hence, higher-order SMC Oumer and Hunde (2015) is an upgraded approach that can attenuate chattering problems and guarantee finite-time convergence. Besides, the combination of Backstepping and SMC is another strategy to enhance the performance by taking advantage of both controllers Thi et al. (2019) and Wang et al. (2020a). In order to solve the phenomenon of "explosion of terms", the Dynamic surface control (DSC) technique has been proposed Tien et al. (2019) and Qinyang et al. (2017), in which multiple sliding surfaces combined with the Backstepping technique and a low-pass filter for each computation step are leveraged. In addition, there are some other effective methods, such as fuzzy techniques, which are capable of estimating virtual signals and minimizing chattering Zhang et al. (2020a).

Model predictive control (MPC) is an advanced control method based on time-domain optimization techniques in presence of constraints Li et al. (2021), Han et al. (2018), Inel et al. (2021), Tian and Wang (2022). Recently, along with the development of computer technology and the availability of models of many engineering subjects, the construction and implementation of MPC controllers in hardware systems is not a challenging problem anymore. Moreover, owing to the capability of explicitly handling hard constraints existing in the system, which are normally neglected in the traditional control methods mentioned above, the MPC method is considered as a potent tool to solve control engineering problems Wen et al. (2018), Song and Huh (2021), and Santos et al. (2019). In Tian and Wang (2022), a novel predictive control compensation method is introduced to effectively handle the random time-delay in a networked control system by using different compensation strategies for input time-delay and output time-delay. The fast implicit generalized predictive control algorithm is employed, which combines the historical output and control variable value to compensate for the time-delay in the input channel. Meanwhile, the feedback loop is added to the control compensator, and the error between the actual control signal and the controller output is predicted to compensate for the time-delay in the output channel, leading to a significant improvement in the system's performance. A novel nonlinear algorithm is developed in Inel et al. (2021) for the trajectory tracking of a planar cable-driven parallel robot based on the finite horizon continuous-time minimization of a quadratic predicted cost function. The main idea of MPC is that, at each sampling instant, it takes the current output measurements, inputs, dynamic states, and mathematical model of the plant to predict the future system states and calculate a consequence of the control signal over a finite horizon by optimizing an objective function subject to some constraints, and then apply only the first element in the sequence to control the system. Nevertheless, as a consequence, the direct relationship between the control signals and input variables is not expressed, making it challenging to analyze the system's stability, especially in nonlinear systems like the parallel robot. Since stability is the most critical characteristic of any closed-loop system, any controller must guarantee this requirement

in the design process. Therefore, a set of stability constraints are normally added to the MPC problem to ensure the stability standard of the closed-loop system. Among many schemes in the literature, the Lyapunov-based model predictive control (LMPC) approach is usually employed because it can explicitly characterize the stability region, and the stability conditions are straightforward to be constructed as well as implemented, which diminishes the complexity of the optimization problem Liu et al. (2017a), Kiani and Mashhadi (2017). The LMPC approach adds some appropriate constraints to the optimization problem based on an auxiliary Lyapunov-based controller and its corresponding Lyapunov function; thus, the robustness and stability of the Lyapunov-based controller can be inherited. In Liu et al. (2017a), a LMPC controller is proposed for non-holonomic mobile robots under input constraints. The auxiliary controller is derived from a global bounded state feedback controller, which satisfies the control input constraints; hence, the contraction condition based on its corresponding Lyapunov function guarantees the recursive feasibility and closed-loop stability of the LMPC problem. Kim et al. (2019) proposed a backstepping controller combined with LMPC, in which the virtual control signal of the first step in the backstepping design procedure is replaced by an optimized solution of LMPC under the input constraints. Therefore, the controller can take advantage of both the backstepping controller in terms of simple and fast calculation and the MPC controller regarding the ability to handle the system constraints.

In the control field, the disturbance is considered an inevitable elementary existing in any engineering system. Hence, it is pivotal to analyze and design a noise compensator to make the controller more stable and robust. Regarding CDS, the noise components frequently occur in many ways Hao et al. (2016), Ramírez-Neria et al. (2015), and Zhengsheng et al. (2021) such as unknown variable forces acting on its actuator's vertical system because of the sudden change of body weight, or the dry and viscous friction force, or the parametric uncertainties of the mathematical model, etc. In Hao et al. (2016), a fast friction approximator derived from the Lyapunov design process is proposed to estimate unknown frictions of each electrical cylinder of a 6-DOF parallel manipulator. Ramírez-Neria et al. (2015) proposed a Generalized Proportional Integral (GPI) observer to estimate the lumped disturbance inputs and the phase variable of linear multivariable output feedback scheme, so the exact information of delta parallel robot system is not necessary. On the other hand, in conventional nonlinear controllers such as Backstepping, SMC, a fuzzy logic controller accompanied by an adaptive law is usually integrated, which utilizes the mathematical characteristics and logic rules to effectively calculate the unknown components and track their change Ji et al. (2020), Godbole et al. (2019). In fuzzy logic controller literature, adaptive law is paramount in adjusting fuzzy parameters since the external disturbance and parameter perturbation typically are unknown and very arbitrarily. In Zhang et al. (2020b), an adaptive fuzzy sliding mode control for the 3-DOF parallel manipulator is proposed, in which the sliding mode controller with its gains are adjusted by the fuzzy system is used to compensate for the parametric uncertainties of the system, and the impact of external disturbances are diminished by adaptation law. Wu et al Wu et al. (2016) presented an H-infinity based on variable structure adaptive fuzzy control for tower crane system under the impacts of external disturbances, parametric uncertainties, and time delay. By combining the adaptive fuzzy control with a variable structure scheme, the system parameters are not required to be known in advance, while the H-infinity control technique rejects the fuzzy errors and disturbance. In addition, in Baigzadehnoe et al. (2017), a fuzzy approximation system with an adaptation law is used to estimate unknown nonlinearities of cooperative robot systems, combined with a backstepping controller to guarantee the boundness of all close-loop signals and the tracking errors converging to desired values.

Inspired by the methods mentioned above, in this paper, an adaptive fuzzy Lyapunov-based model predictive controller is proposed for the CDS taking into consideration the system's constraints and the presence of external disturbances and model uncertainties to ensure the tracking performance of 4 DOF car driving simulations. The paper contributions can be summarized as follows:

1. The proposed method is able to cope with the problem of controller design for the CDS considering the input and system constraints which are typically neglected in many studies, especially conventional nonlinear controllers Lu et al. (2018), Ji et al. (2020), and Tian (2021). Theoretically, if these constraints are not adequately handled in the control formulation, the overall stability cannot be guaranteed; moreover, the signal generated by the controller can exceed the system actuator capacity if control parameters are not moderately determined. By employing the MPC controller, all the constraints are explicitly expressed and solved in the optimizing process, leading to improved performance and the robustness of the tracking problem for the CDS. Therefore, the proposed controller is more efficient and effective in ensuring stability in the presence of practical constraints.
2. The proposed controller also has an ability to deal with the stability problem of traditional nonlinear MPC, leading to the system's stability being explicitly analyzed, owning a stable feedback controller and its corresponding Lyapunov function, and thus the sufficient conditions to guarantee the recursive feasibility and closed-loop stability for MPC problems are explicitly derived without local linearization step as in Christofides et al. (2011). Based on this pivotal property, the guaranteed region of attraction is critically described. Moreover, the Lyapunov control law used for the contraction condition of LMPC is designed based on an adaptive nonlinear fuzzy controller. Hence, it takes advantage of the two controllers, including Backstepping and Sliding Mode Control, in the system stability assurance. Furthermore, the adaptive rule with online learning capacity significantly improves the quality of the Lyapunov control, especially in terms of disturbances, and thus it enhances the performance of the generated signal from MPC.
3. The Fuzzy logic system is designed accompanied by an adaptive updated law for the Lyapunov-based MPC controller, which can approximate the unknown external disturbances and uncertain parameters to enhance predictive quality. Typically, the MPC performance significantly depends on the accuracy of the predictive model obtained from the system's mathematically modeling process. Therefore, unmodelled elements remarkably take adverse impacts on the system behavior. Hence, the controller can ensure the control quality even in the presence of unmodelled elements. Compared to Zhang et al. (2020a), Xu et al. (2018), and Wang et al. (2020b), the fuzzy outputs are illustrated to verify the accuracy of estimated values, as well as its efficiency when being integrated with the LMPC controller.

The remainder of this paper is organized as follows: The kinematic and dynamic model of the car-driving system under external disturbances are represented in Section 2. In Section 3, the Lyapunov-based nonlinear model predictive control formulation is introduced. Next, Section 4 illustrates the fuzzy approximation system to estimate the external disturbance, then constructs the contraction condition for the LMPC problem via an adaptive fuzzy backstepping sliding mode control scheme. After that, the system's stability under the proposed controller is analyzed in detail in Section 5. Simulation results and comparisons are highlighted in Section 6. Finally, the paper is wrapped up by some conclusive remarks in Section 7.

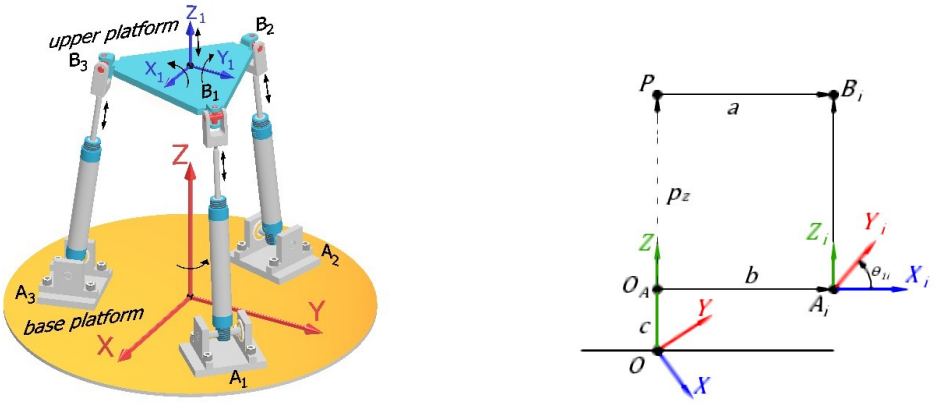

Figure 1. (a) Robot's coordinates; (b) Vector diagram of CDS. Manh et al. (2021)

The driving simulator problem formulation

Kinematic modeling

Define vector $p = \begin{bmatrix} p_z & \alpha & \beta & \gamma \end{bmatrix}^T$ as the system state vector where: p_z is the vertical position and α, β, γ are rotation angular about OX, OY, OZ axes, respectively. Vector $q = \begin{bmatrix} l_1 & l_2 & l_3 & \gamma \end{bmatrix}^T$ describes the piston's length and OZ rotation angular where c is the distance between origin O and base platform's O_A, a, b are the radius of upper and base platforms, respectively.

The 4DOF Car driving simulator can be shown in Fig. 1. The vector equation of 4DOF Car driving simulator where $i = 1, 2, 3$ can be written as:

$$\overrightarrow{A_iB_i} = \overrightarrow{OP} + \overrightarrow{PB_i} - \overrightarrow{O_AA_i} - \overrightarrow{OO_A} \tag{1}$$

Denote $A_i, i = 1, 2, 3$ are the coordinates in the local coordinate O_AXYZ associated with the base panel's center with:

$$A_{ibase} = \begin{bmatrix} b\cos(\theta_i) & b\sin(\theta_i) & 0 \end{bmatrix}^T \tag{2}$$

and $B_i, i = 1, 2, 3$ are the coordinates in the local coordinate $PX_1Y_1Z_1$ associated with the base panel's center with

$$B_{iupper} = \begin{bmatrix} a\cos(\theta_i) & a\sin(\theta_i) & 0 \end{bmatrix}^T \tag{3}$$

where $\theta_1 = \dfrac{\pi}{3}$, $\theta_2 = \pi$ and $\theta_3 = \dfrac{5\pi}{3}$ are the distributed angles of pistons on base platform.

Besides, in the global coordinate, the center points of the base and upper panel are $O_A = \begin{bmatrix} 0 & 0 & c \end{bmatrix}^T$ and $p_{de} = \begin{bmatrix} 0 & 0 & p_z \end{bmatrix}^T$.

Fixed coordinates of A_i and B_i are $A_i = T_AA_{ibase} + O_A$ and $B_i = T_PB_{iupper} + p_{de}$, which can be obtained as follows:

$$T_A = \begin{bmatrix} \cos\gamma & -\sin\gamma & 0 \\ \sin\gamma & \cos\gamma & 0 \\ 0 & 0 & 1 \end{bmatrix}$$

$$T_P = \begin{bmatrix} \cos\gamma & -\sin\gamma & 0 \\ \sin\gamma & \cos\gamma & 0 \\ 0 & 0 & 1 \end{bmatrix} \begin{bmatrix} \cos\beta & 0 & \sin\beta \\ 0 & 1 & 0 \\ \sin\beta & 0 & \cos\beta \end{bmatrix} \begin{bmatrix} 1 & 0 & 0 \\ 0 & \cos\alpha & -\sin\alpha \\ 0 & \sin\alpha & \cos\alpha \end{bmatrix}$$

Finally, the length of the robot's legs is computed as

$$l_i = \|A_i B_i\|_2 \tag{4}$$

where $A_i B_i = B_i - A_i$. From (4), q can be computed from p.

System dynamics modeling

According to Tien et al. (2019), Manh et al. (2021), the dynamic model based on Euler-Lagrange form is described as:

$$M\ddot{q} + C\dot{q} + G + D = F \tag{5}$$

where M is the mass matrix, C is the Coriolis and centrifugal matrix determined from the mass matrix, D is the aggregation of generalized force and model uncertainties caused by the potential energy and unknown system elements. The control signal vector is defined by $F = \begin{bmatrix} F_1 & F_2 & F_3 & \tau_\gamma \end{bmatrix}^T$. Besides:

$$M = \begin{bmatrix} m_2 + m_{dc} + \frac{m_p}{9} + \frac{I_{py}}{4a^2} & \frac{m_p}{9} & \frac{m_p}{9} & 0 \\ \frac{m_p}{9} & m_2 + m_{dc} + \frac{m_p}{9} + \frac{I_{px}}{12a^2} & \frac{m_p}{9} & 0 \\ \frac{m_p}{9} & \frac{m_p}{9} & m_2 + m_{dc} + \frac{m_p}{9} & 0 \\ 0 & 0 & 0 & I_\gamma \end{bmatrix} \tag{6}$$

with m_1 is the mass of the covering of piston, m_2 is the mass of the pistons, m_{dc} is the mass of the motor on the cylinders and m_p is the mass of the mobile panels, I_{px}, I_{py}, and I_γ are the inertia of the mobile panels along Ox, O_y, and Oz, respectively. And:

$$C = \begin{bmatrix} \frac{15 I_{py} i_1^2}{4a^4} & 0 & 0 & 0 \\ 0 & \frac{5 I_{px} i_2^2}{12a^4} & 0 & 0 \\ 0 & 0 & 0 & 0 \\ 0 & 0 & 0 & 0 \end{bmatrix} \tag{7}$$

$$G = \left(m_2 + \frac{m_p}{3}\right) g \begin{bmatrix} 1 & 1 & 1 & 0 \end{bmatrix}^T \tag{8}$$

with $g = 9.8$ m/s^2 is the gravitational acceleration. The disturbance is added to the dynamic system in the following form:

$$D = \begin{bmatrix} d_1 & d_2 & d_3 & d_4 \end{bmatrix}^T \tag{9}$$

For the given system, nonlinear model-based controllers, including Backstepping and SMC, can achieve the control target of reference tracking provided that accurate mathematical model is available. A modern control method using radial basis function neural network with Lyapunov based adaptive law as in Manh et al. (2021) not only copes with this kind of problem but eliminates the drawbacks of these controllers. However, the constraints of system states, control inputs, and experimental parameters are not considered, and thus the actuator constraint and even the stability cannot be satisfied.

In practice, the input constraints include the maximum and minimum forces of three pistons as well as the limited rotation torque mobile panel. In addition, the system constraints are expressed in the stroke length of three pistons and the rotation angle of the model panel. In our work, all these unavoidable constraints are taken into consideration.

Lyapunov-based model predictive control

The system constraints are considered in the control signal computation by the optimization progress of the MPC controller. The advantage of the LMPC method is that it can explicitly handle the input and state constraints in the control design step and simultaneously can predict and evaluate the future system states in the optimization step to induce satisfied control input for the current step accordingly. In addition, based on the Lyapunov stability theory, the stability of the nonlinear system is guaranteed. Hence, in this section, the nonlinear Lyapunov-based Model predictive control (LMPC) for the CDS problem is presented in detail. The summary of CDS dynamic model:

$$F = M\left(q,\dot{q}\right)\ddot{q} + C\left(q,\dot{q}\right)\dot{q} + G + D \tag{10}$$

The equation (10) can be rewritten as:

$$\ddot{q} = M^{-1}\left(q,\dot{q}\right)\left(F - C\left(q,\dot{q}\right)\dot{q} - G\right) - N \tag{11}$$

with $N = M^{-1}D$. Let $x = \begin{bmatrix} q \\ \dot{q} \end{bmatrix}$, the dynamic model of CDS can be expressed in the following form:

$$\dot{x} = \begin{bmatrix} \dot{q} \\ M^{-1}\left(q,\dot{q}\right)\left(F - C\left(q,\dot{q}\right)\dot{q} - G\right) - N \end{bmatrix} = f\left(x\right) \tag{12}$$

Let $\tilde{x} = x - x_d$ be the state vector, $u = F - F_d$ be the control error. The nonlinear model predictive controller for car driving simulator tracking problem can be formulated as follows

$$F = \arg\min_{F\in\Omega_F} J = \arg\min_{F\in\Omega_F} \left\|\tilde{x}\left(t_k + T\right)\right\|_P^2 + \int_{t_k}^{t_k+T} \left\|\tilde{x}\left(t\right)\right\|_Q^2 + \left\|u\left(t\right)\right\|_R^2 dt \tag{13}$$

subject to

$$\dot{x}\left(t\right) = f\left(x\left(t\right), F\left(t\right)\right)\ \forall\, t \in [t_k; t_k + T]; \tag{14a}$$
$$x\left(t_k\right) = x_o\ \forall\, t \in [t_k; t_k + T]; \tag{14b}$$
$$\left|x\left(t\right)\right| \leq x_{max}; \tag{14c}$$
$$\left|F\left(t\right)\right| \leq F_{max} \tag{14d}$$

In which, Q, R, and P are positive weighting matrices. T is the prediction horizon, t_k is hte current time instant. However, because of the finite prediction horizon, the complex offline design procedure is usually carried out to ensure the stability of the closed-loop system when applying an optimal solution. For nonlinear system, the standard MPC implicitly define the region of attraction (ROA) by local linearization. In order to overcome this problem, the Lyapunov-based strategy is employed to formulate the LMPC problem by introducing a contraction constraint to the original MPC problem.

$$\frac{\partial V}{\partial x} f\left(x\left(t_k\right), F\left(t_k\right)\right) \leq \frac{\partial V}{\partial x} f\left(x\left(t_k\right), h\left(q\left(t_k\right)\right)\right), \quad \forall t \in \left[t_k; t_k + T\right] \tag{15}$$

where $h\left(\cdot\right)$ is the auxiliary Lyapunov-based controller corresponding to Lyapunov function $V\left(\cdot\right)$. This contractive constraint guarantee that the LMPC inherits the stability and robustness properties of Lyapunov-based controller $h\left(\cdot\right)$ irrespective of the length of the prediction horizon, and also explicitly characterize the ROA where the stability is guaranteed.

The LMPC control algorithm for CDS trajectory problem is summarized in Algorithm 1

Algorithm 1:

1. Input the objective function J
2. Measure the current state $x\left(t\right)$
3. Solve the LMPC problem (13) with $x\left(t\right) = x\left(t_0\right)$, resulting the sub-optimal solution F_{sub}
4. Perform F_{sub} for only one sample period $F\left(t\right) = F_{sub}$ for $t \in \left[t_k, t_{k+1}\right]$
5. Repeat from step 2 in the next sampling time

Remark 1. In Algorithm 1, the suboptimal solutions are acceptable for the nonlinear MPC algorithm. The iterative methods can ensure that the solution to (13) is locally optimal. Moreover, the number of iterations is restricted in real-time performance due to limited computational resources. However, as can be seen in the later section, neither the recursive feasibility nor closed-loop stability of the LMPC algorithm depends on the optimal global solution. Therefore, it is flexible to trade off the computational time and algorithm accuracy without destabilizing the tracking control.

Closed loop Lyapunov-based controller design

This section presents the fuzzy approximation mechanism to estimate the external disturbance and then illustrates the procedure to construct the auxiliary controller using the backstepping sliding mode control technique with the estimated disturbance value and adaptation law. Subsequently, the detail of the contraction condition for the MPC problem is derived.

External disturbance estimation

Assumption 0.1. *The external disturbance D is bounded.*

Due to the fact that the external disturbance D is undefined, as well as N, it can be approximated by fuzzy logic system with the input vector $\tilde{x} = \begin{bmatrix} q - q_d \\ \dot{q} - \dot{q}_d \end{bmatrix} = \left(\tilde{x}_1, \tilde{x}_2, \tilde{x}_3, \tilde{x}_4, \tilde{x}_5, \tilde{x}_6, \tilde{x}_7, \tilde{x}_8\right)^T$. The output

of fuzzy system using the strategy of singleton fuzzifier, product inference engine, and center-average defuzzifier can be inferred as

$$y = \frac{\sum_{i=1}^{M} \prod_{j=1}^{8} \mu_{X_j^i}(\tilde{x}_j)\, y_i}{\sum_{i=1}^{M} \prod_{j=1}^{8} \mu_{X_j^i}(\tilde{x}_j)} = W^T \xi(\tilde{x}) \tag{16}$$

where $\mu_{X_j^i}$ is the membership function of the i^{th} fuzzy set for the j^{th} input $\tilde{x}_j$, $\boldsymbol{W} = [y_1, ..., y_M]^T$ is the adjustable parameters vector, $\zeta(x) = [\zeta_1, ..., \zeta_M]^T$ with $\zeta_i = \dfrac{\prod_{j=1}^{8} \mu_{X_j^i}(\tilde{x}_j)}{\sum_{i=1}^{M} \prod_{j=1}^{8} \mu_{X_j^i}(\tilde{x}_j)}$, being fuzzy basis function, M is the number of IF-THEN rules. Therefore, the approximation of N can be expressed as

$$\hat{N} = W^T \zeta(x) \tag{17}$$

Assuming that $\mathbf{x}$ and $\mathbf{W}$ are constrained in the compact set Ω_x, Ω_W respectively with $\Omega_x = \left\{\boldsymbol{x} | \underline{\varsigma}_x \leq \boldsymbol{x} \leq \bar{\varsigma}_x\right\}$, $\Omega_W = \left\{\boldsymbol{W} | \underline{\varsigma}_W \leq \boldsymbol{W} \leq \bar{\varsigma}_W\right\}$, and there exists optimal parameters $\mathbf{W}^*$ such that

$$\boldsymbol{W}^* = \arg\min_{W} \left\{ \sup_{x \in \Omega_x} \left| N(\boldsymbol{x}) - \boldsymbol{W}^T \zeta_n(\boldsymbol{x}) \right| \right\} \tag{18}$$

Define the estimated parameter errors as $\tilde{\boldsymbol{W}} = \boldsymbol{W} - \boldsymbol{W}^*$, the error between the optimal value with approximation value can be written as

$$\tilde{N} = \hat{N} - N^* = (W - W^*)\, \zeta(x) \tag{19}$$

Remark 2. Because fuzzy basis functions $\zeta_i(x) \in [0, 1], i = 1, \bar{M}$ and the adjustable parameters vector W are constrained in compact set Ω_W, $\hat{N}$ is bounded satisfying $0 \leq \left|\hat{N}\right| \leq \bar{n}$. Besides, the external disturbance D is bounded and N^* is the optimal value of D, hence N^* is also bounded, leading to $0 \leq \left|\tilde{N}\right| \leq \kappa$.

Adaptive fuzzy Backstepping SMC design

To construct contraction constraint, the adaptive fuzzy backstepping SMC (BSMCF) is employed to create the auxiliary controller $h(\cdot)$ and its corresponding Lyapunov function. Firstly, the tracking error is defined as $\xi_1 = q - q_d$. From that, the virtual control is chosen as the derivative of for the stabilization of q for the stabilization ξ_1. Considering the following Lyapunov candidate function

$$V_1 = \frac{1}{2} \xi_1^T \xi_1 \tag{20}$$

Its derivative is

$$\dot{V}_1 = \xi_1^T \dot{\xi}_1 = \xi_1^T (\dot{q} - \dot{q}_d) \tag{21}$$

The objective of this step is to find a control law $\alpha(q)$ with $\alpha(0) = 0$ such that when $\dot{q} = \alpha(q)$ then $\dot{V}_1(q) < 0$. From (21), $\alpha(q)$ can have the following form

$$\alpha = \dot{q}_d - K_1 \xi_1 \tag{22}$$

where $K_1 = diag\left(k_{11}, k_{12}, k_{13}, k_{14}\right)$ is positive gain. Substituting $\alpha\left(q\right)$ to (21) yields

$$\dot{V}_1 = -\xi_1^T K_1 \xi_1 \tag{23}$$

Next, denote the error between $\dot{q}$ and $\alpha\left(q\right)$ as $\xi_2 = \dot{q} - \alpha$. Taking the derivative of ξ_2 gives:

$$\begin{aligned} \dot{\xi}_2 = \ddot{q} - \dot{\alpha} &= M^{-1}F - M^{-1}\left(C\dot{q} + G\right) - M^{-1}D \\ &= M^{-1}F - M^{-1}\left(C\dot{q} + G\right) - N \end{aligned} \tag{24}$$

with $N = M^{-1}D$. To formulate the control signal, the second Lyapunov candidate function is defined to guarantee global stability as follows.

$$V = V_1 + \frac{1}{2}\xi_2^T\xi_2 + \frac{1}{2}\text{trace}\left(\tilde{W}^T\Gamma^{-1}\tilde{W}\right) \tag{25}$$

Its derivative is

$$\dot{V} = \dot{V}_1 + \xi_2^T\left(M^{-1}F - M^{-1}\left(C\dot{q} + G\right) - N\right) + \text{trace}\left(\tilde{W}^T\Gamma^{-1}\left(-\dot{\hat{W}}\right)\right) \tag{26}$$

The designed control signal F includes two components: the equivalent control F_{eq} which is responsible for keeping the system states on the sliding surface, and the switching control F_{sw} forcing the system to an equilibrium point.

$$\begin{aligned} F_{eq} &= C\dot{q} + G + M\hat{N} - M\left(\xi_1 - \dot{\alpha}\right) \\ F_{sw} &= -M\left(k_2\text{sign}\left(\xi_2\right) + k_3\xi_2\right) \\ F &= F_{eq} + F_{sw} = C\dot{q} + G + M\hat{N} - M\left(\xi_1 - \dot{\alpha}\right) - M\left(k_2\text{sign}\left(\xi_2\right) + k_3\xi_2\right) \end{aligned} \tag{27}$$

Substituting (27) to (24) yields

$$\begin{aligned} \dot{\xi}_2 = \ddot{q} - \dot{\alpha} &= -\left(\xi_1 + k_2\text{sign}\left(\xi_2\right) + k_3\xi_2\right) + \hat{N} - N \\ &= -\left(\xi_1 + k_2\text{sign}\left(\xi_2\right) + k_3\xi_2\right) + \left(\hat{N} - N^* + N^* - N\right) \\ &= -\left(\xi_1 + k_2\text{sign}\left(\xi_2\right) + k_3\xi_2\right) + \tilde{W}^T h + \varepsilon \end{aligned} \tag{28}$$

with $\varepsilon = N^* - N$. The adaptive rule is selected as

$$\dot{\hat{W}} = \Gamma h \xi_2^T \tag{29}$$

Using (29) and (28), $\dot{V}$ becomes:

$$\begin{aligned} \dot{V} &= \dot{V}_1 + \xi_2^T\left(-\xi_1 + \tilde{W}^T h + \varepsilon - k_2\text{sign}\left(\xi_2\right) - k_3\xi_2\right) + \text{trace}\left(\tilde{W}^T\Gamma^{-1}\left(-\dot{\hat{W}}\right)\right) \\ &= -\xi_1^T k_1\xi_1 - \xi_2^T k_2\text{sign}\left(\xi_2\right) - \xi_2^T k_3\xi_2 + \xi_2^T\varepsilon + \text{trace}\left(\tilde{W}^T\Gamma^{-1}\left(\Gamma\xi_2^T h - \dot{\hat{W}}\right)\right) \\ &= -\xi_1^T k_1\xi_1 - \xi_2^T k_2\text{sign}\left(\xi_2\right) - \xi_2^T k_3\xi_2 + \xi_2^T\varepsilon \end{aligned} \tag{30}$$

If k_2 is chosen such that $k_2 > \varepsilon$, then

$$\dot{V} \leq -\xi_1^T k_1\xi_1 - \xi_2^T k_3\text{sign}\left(\xi_2\right) - \left|\xi_2\right|^T\left(k_2 - \left|\varepsilon\right|\right) \leq 0 \tag{31}$$

Therefore, the system is global asymptotical stability under the control input (27) and the adaptive law (29)

Contraction condition construction

From Backstepping SMC design procedure above, the auxiliary controller is

$$h\left(x\right)=F_{eq}+F_{sw}=C\dot{q}+G+M\hat{N}-M\left(\xi_1-\dot{\alpha}\right)-M\left(k_2\text{sign}\left(\xi_2\right)+k_3\xi_2\right) \tag{32}$$

with its corresponding Lyapunov function

$$\dot{V}_{BSMC}=-\xi_1^T k_1\xi_1-\xi_2^T k_2\text{sign}\left(\xi_2\right)-k_2^T k_3\xi_2+\xi_2^T\varepsilon \tag{33}$$

The contraction condition for LMPC problem can be expressed as $\dot{V}_{LMPC}\leq\dot{V}_{BSMC}$. Considering the $\dot{V}_{lMPC}$ as follow:

$$\begin{aligned}\dot{V}_{LMPC}&=\xi_1^T\xi_2-\xi_1^T k_1\xi_1+\text{trace}\left(\tilde{W}^T\Gamma^{-1}\left(-\dot{\hat{W}}\right)\right)+\xi_2^T\left(M^{-1}F-M^{-1}\left(C\dot{q}+G\right)-M^{-1}D-\dot{\alpha}\right)\\&=\xi_1^T\xi_2-\xi_1^T k_1\xi_1+\text{trace}\left(\tilde{W}^T\Gamma^{-1}\left(-\dot{\hat{W}}\right)\right)+\xi_2^T\left(M^{-1}F-M^{-1}\left(C\dot{q}+D+\hat{N}\right)-\dot{\alpha}\right)\\&\quad-\xi_2^T M^{-1}\left(N-N^*+N^*-\hat{N}\right)\\&=\xi_1^T\xi_2-\xi_1^T k_1\xi_1+\text{trace}\left(\tilde{W}^T\Gamma^{-1}\left(-\dot{\hat{W}}\right)\right)+\xi_2^T\left(M^{-1}F-M^{-1}\left(C\dot{q}+D+\hat{N}\right)-\dot{\alpha}\right)+\xi_2^T\varepsilon-\xi_2^T\tilde{W}^T\end{aligned} \tag{34}$$

The adaptive law used for LMPC is selected as (29). Therefore:

$$\dot{V}_{LMPC}=\xi_1^T\xi_2-\xi_1^T k_1\xi_1+\xi_2^T\varepsilon+\xi_2^T\left(M^{-1}F-M^{-1}\left(C\dot{q}+D+\hat{N}\right)-\dot{\alpha}\right) \tag{35}$$

Finally, the detailed contraction condition for LMPC can be expressed as

$$\begin{aligned}&\xi_1^T\left(t_k\right)\xi_2\left(t_k\right)-\xi_1^T\left(t_k\right)k_1\xi_1\left(t_k\right)\\&+\xi_2^T\left(t_k\right)\left(M^{-1}\left(q\left(t_k\right)\right)F\left(t_k\right)^{-1}-M^{-1}\left(q\left(t_k\right)\right)\left(C\left(q\left(t_k\right),\dot{q}\left(t_k\right)\right)\dot{q}\left(t_k\right)+D\left(t_k\right)+\hat{N}\left(t_k\right)\right)-\dot{\alpha}\left(t_k\right)\right)\\&\leq-\xi_1^T\left(t_k\right)k_1\xi_1\left(t_k\right)-\xi_2^T\left(t_k\right)k_2\text{sign}\left(\xi_2\left(t_k\right)\right)-\xi_2\left(t_k\right)k_3\xi_2\left(t_k\right),\forall t\in\left[t_k;t_k+T\right]\end{aligned} \tag{36}$$

Remark 3. In order to ensure that the adaptation parameters $\hat{\mathbf{W}}$ with adaptive adjustment law $\dot{\hat{\mathbf{W}}}$ are bounded for all $t\geq 0$ in the constraint set Ω_L, the following projection function are used

$$\dot{\hat{\boldsymbol{W}}}=\begin{cases}0 & \text{if } \hat{\boldsymbol{W}}>\bar{\zeta}_W \text{ and } \dot{\hat{\boldsymbol{W}}}>0\\0 & \text{if } \hat{\boldsymbol{W}}<\bar{\zeta}_W \text{ and } \dot{\hat{\boldsymbol{W}}}<0\\\dot{\hat{\boldsymbol{W}}} & \text{otherwise}\end{cases} \tag{37}$$

Remark 4. The fuzzy logic system approximates the external disturbance with adaptive law (29) in each sample time, and its value is used for the LMPC controller to predict state trajectory in the horizon T_h. However, in some cases, the value of disturbance change erratically and rapidly; it takes time for the fuzzy approximation system to adjust the current estimated value to the accurate one. Hence, if prediction horizon T_h and the frequency of disturbance f_d can satisfy $T_h f_d<1$, the approximation error is ensured to converge to a small region around the origin.

Stability analysis for the LMPC

In this section, the recursive feasibility and the closed-loop stability of the LMPC problem are considered. The following assumptions are set in advance

Assumption 0.2. *The reference signals are smooth and upper bounded*

$$\left\|q_d\left(t\right)\right\|_\infty \leq \bar{q}_d, \left\|\dot{q}_d\left(t\right)\right\|_\infty \leq \bar{q}_{d1}, \left\|\ddot{q}_d\left(t\right)\right\|_\infty \leq \bar{q}_{d2} \tag{38}$$

Assumption 0.3. *Three pistons have the same capacity* $F_{1max} = F_{2max} = F_{3max} = P_{max}$ *and* $\tau_\gamma \leq \tau_{max}$

Theorem 0.4. *If the following relation can be satisfied:*

$$\bar{c}\bar{q}_{d1} + \bar{m}\bar{q}_{d2} + \left\|\chi\left(0\right)\right\|_2\left(1+\bar{c}\right) + \bar{g} + \bar{m} + \bar{k}_{2max} + \left(\bar{k}_{1max}\left(\bar{k}_{1max}+1+\bar{c}\right) + \bar{k}_{3max}\right)\left\|\chi\left(0\right)\right\|_2 \leq f_{max} \tag{39}$$

and

$$I_\gamma\left(\bar{n} + \bar{q}_{d2} + \bar{k}_{1max}\left(\bar{k}_{1max}+1\right)\left\|\chi\left(0\right)\right\|_2 + \bar{k}_{2max} + \bar{k}_{3max}\left\|\chi\left(0\right)\right\|_2 + \left\|\chi\left(0\right)\right\|_2\right) \leq \tau_{max} \tag{40}$$

then the LMPC admit recursive feasibility for all $t \geq 0$.

Proof. It is important to note that given the current system state $x\left(t\right)$, $h\left(x\right)$ is always feasible for the LMPC problem if $h\left(x\right) \leq F_{max} = \left[F_{1max}, F_{2max}, F_{3max}, \tau_{\gamma max}\right]^T$ can be satisfied.

Let $\chi = \begin{bmatrix} \xi_1 \\ \xi_2 \end{bmatrix}$, consider the Lyapunov function $V_e = V_1 + \frac{1}{2}\xi_2^T\xi_2 = \frac{1}{2}\chi^T\Xi\chi$ with $\Xi = \begin{bmatrix} I & 0 \\ 0 & I \end{bmatrix}$. Its derivative is

$$\dot{V}_e = \dot{V}_1 + \xi_2^T\left(-\xi_1 - k_2\text{sign}\left(\xi_2\right) - k_3\xi_2\right) + \xi_2^T\left(\hat{N} - N\right) \tag{41}$$

If the auxiliary controller $h\left(x\right)$ is implemented, substitute (28) to (41) yields:

$$\begin{aligned}
\dot{V}_e &= -\xi_1^T k_1\xi_1 - \xi_2^T k_2\text{sign}\left(\xi_2\right) - \xi_2^T k_3\xi_2 + \xi_2^T\left(\hat{N} - N\right) \\
&< -\xi_1^T k_1\xi_1 - \xi_2^T k_3\xi_2 - \left|\xi_2^T\right|\left(k_2 - \left|\hat{N} - N\right|\right) \\
&= -\xi_1^T k_1\xi_1 - \xi_2^T k_3\xi_2 - \left|\xi_2^T\right|\left(k_2 - \left|\hat{N} - N^* + N^* - N\right|\right) \\
&\leq -\xi_1^T k_1\xi_1 - \xi_2^T k_3\xi_2 - \left|\xi_2^T\right|\left(k_2 - \left|\varepsilon + \kappa\right|\right)
\end{aligned} \tag{42}$$

If k_2 is opted such that $k_1 > \varepsilon + \kappa$, then $\dot{V}_e \leq 0$, which means $\left\|\chi\left(t\right)\right\|_2 \leq \left\|\chi\left(0\right)\right\|_2$. Moreover, $\left\|\xi_1\right\|_\infty \leq \left\|\chi\right\|_\infty$, $\left\|\xi_2\right\|_\infty \leq \left\|\chi\right\|_\infty$. Let $k_{1max} = \left\|K_1\right\|_\infty$ and $k_{2max} = \left\|K_2\right\|_\infty$, then the following inequation is hold

$$\begin{aligned}
\left\|\dot{\xi}_1\right\|_\infty = \left\|\xi_2 - K_1\xi_1\right\|_\infty &\leq \left\|\xi_2\right\|_\infty + k_{1max}\left\|\xi_1\right\|_\infty \\
&\leq \left(1 + k_{1max}\right)\left\|\chi\right\|_\infty \\
&\leq \left(1 + k_{1max}\right)\left\|\chi\left(0\right)\right\|_\infty \\
&\leq \left(1 + k_{1max}\right)\left\|\chi\left(0\right)\right\|_2
\end{aligned} \tag{43}$$

Since $\|\dot{q}\|_\infty = \left\|\dot{\xi}_1 + \dot{q}_d\right\|_\infty \leq \left\|\dot{\xi}_1\right\|_\infty + \|\dot{q}_d\|_\infty$, from (38) and (43) gives:

$$\|\dot{q}(t)\|_\infty \leq \bar{q}_{d1} + (1+k_1)\|\chi(0)\|_2 \tag{44}$$

Next, from (38) and (22)

$$\begin{aligned} &\dot{\alpha} = \ddot{q}_d - k_1\dot{\xi}_1 \\ &\|\dot{\alpha}\|_\infty = \left\|\ddot{q}_d - k_1\dot{\xi}_1\right\|_\infty \leq \bar{q}_{d2} + k_{1max}(k_{1max}+1)\|\chi(0)\|_2 \end{aligned} \tag{45}$$

Considering the control input of three pistons F_{ps} as follow:

$$F_{ps} = [F_1, F_2, F_3]^T = Ah(x) \tag{46}$$

with $A = \begin{bmatrix} 1 & 0 & 0 & 0 \\ 0 & 1 & 0 & 0 \\ 0 & 0 & 1 & 0 \end{bmatrix}$. Substituting (32) to (46) gives:

$$\begin{aligned} F_{ps} = A\Big(&C\dot{q} + G + M\hat{N} - M(\xi_1 - \dot{\alpha}) \\ &-M(k_2\text{sign}(\xi_2) + k_3\xi_2)) \\ &= C_{ps}\dot{q} + G_{ps} + M_{ps}\hat{N} - M_{ps}(\xi_1 - \dot{\alpha}) \\ &- M_{ps}(k_2\text{sign}(\xi_2) + k_3\xi_2) \end{aligned} \tag{47}$$

with

$$M_{ps} = \begin{bmatrix} m_2 + m_{dc} + \frac{m_p}{9} + \frac{I_{py}}{4a^2} & \frac{m_p}{9} & \frac{m_p}{9} & 0 \\ \frac{m_p}{9} & m_2 + m_{dc} + \frac{m_p}{9} + \frac{I_x}{12a^2} & \frac{m_p}{9} & 0 \\ \frac{m_p}{9} & \frac{m_p}{9} & m_2 + m_{dc} + \frac{m_p}{9} & 0 \end{bmatrix} \tag{48}$$

$$C_{ps} = \begin{bmatrix} \frac{15I_{py}\dot{l}_1^2}{4a^4} & 0 & 0 & 0 \\ 0 & \frac{6I_{px}\dot{l}_2^2}{12a^4} & 0 & 0 \\ 0 & 0 & 0 & 0 \end{bmatrix}; G_{ps} = \left(m_2 + \frac{m_p}{3}\right) g \begin{bmatrix} 1 \\ 1 \\ 1 \end{bmatrix} \tag{49}$$

Thus:

$$\|M_{ps}\|_\infty = \frac{m_p}{3} + m_2 + m_{dc} + \max\left\{\frac{I_{py}}{4a^2}, \frac{I_{px}}{12a^2}\right\} = \bar{m} < \infty \tag{50}$$

$$\begin{aligned}\|C_{ps}\|_\infty &= \max\left\{\frac{15I_{py}\dot{l}_1^2}{4a^4}, \frac{5I_{px}\dot{l}_2^2}{12a^4}\right\} \\ &\leq \max\left\{\frac{15I_{py}}{4a^4}, \frac{5I_{px}}{12a^4}\right\}\|q\|_\infty^2 \\ &\leq \max\left\{\frac{15I_{py}}{4a^4}, \frac{5I_{px}}{12a^4}\right\}\left(\bar{q}_{d1} + (1+k_1)\|\chi(0)\|_2\right)^2 = \bar{c}\end{aligned} \tag{51}$$

$$\begin{aligned}\|G_{ps}\|_\infty &= \left\|\left(m_2 + \frac{m_p}{3}\right) g\,[1,1,1]^T\right\|_\infty \\ &= \left(m_2 + \frac{m_p}{3}\right) g = \bar{g} < \infty\end{aligned} \tag{52}$$

Therefore, taking infinity norm on both sides of (47) yields

$$\begin{aligned}\|F_{ps}\|_\infty &= \left\|C_{ps}\dot{q} + G_{ps} + M_{ps}\hat{N} - M_{ps}(\xi_1 - \dot{\alpha}) - M_{ps}(k_2\text{sign}(\xi_2) + k_3\xi_2)\right\|_\infty \\ &\leq \|C_{ps}\dot{q}\|_\infty + \|G_{ps}\|_\infty + \left\|M_{ps}\hat{N}\right\|_\infty + \|M_{ps}\dot{\alpha}\|_\infty + \|M_{ps}(k_2\text{sign}(\xi_2) + k_3\xi_2 + \xi_1)\|_\infty \\ &\leq \bar{c}\left(\bar{q}_{d1} + \left(1 + \bar{k}_{1max}\right)\|\chi(0)\|_2\right) + \bar{g} + \bar{m}\bar{n} + \bar{m}\left(\bar{q}_{d2} + \bar{k}_{1max}\left(\bar{k}_{1max} + 1\right) + \bar{k}_{3max} + 1 + \bar{c}\left(1 + \bar{k}_{max}\right.\right. \\ &= \bar{c}\bar{q}_{d1} + \bar{d} + \bar{m}\left(\bar{q}_{d2} + \bar{k}_{2max} + \bar{n}\right) + \left(\bar{k}_{1max}\left(\bar{k}_{1max} + 1\right) + \bar{k}_{3max} + 1 + \bar{c}(1 + k_{1max})\right)\|\chi(0)\|_2\end{aligned} \tag{53}$$

In term of control input τ_γ to rotate the mobile panels, τ_γ can be represented as follow:

$$\tau_\gamma = Bh(x) \tag{54}$$

with $B = [0,0,0,1]$. Substituting (32) to (54) yields:

$$\begin{aligned}\tau_\gamma = B\Big(&C\dot{q} + G + M\hat{N} - M(\xi_1 - \dot{\alpha}) \\ &-M(k_2\text{sign}(\xi_2) + k_3\xi_2)) \\ &= M_\gamma\hat{N} - M_\gamma(\xi_1 - \dot{\alpha}) - M_\gamma(k_2\text{sign}(\xi_2) + k_3\xi_2)\end{aligned} \tag{55}$$

with $M_\gamma = [0,0,0,I_\gamma]$. Therefore, taking infinity norm on both sides of (55) yields:

$$\begin{aligned}\|\tau_\gamma\|_\infty &= \left\|M_\gamma\hat{N} - M_\gamma(\xi_1 - \dot{\alpha}) - M_\gamma(k_2\text{sign}(\xi_2) + k_3\xi_2)\right\|_\infty \\ &\leq \|M_\gamma\|_\infty\left(\bar{n} + \bar{q}_{d2} + \bar{k}_{1max}\left(k_{1max} + 1\right)\|\chi(0)\|_2 . + \bar{k}_{2max} + \bar{k}_{3max}\|\chi(0)\|_2 + \|\chi(0)\|_2\right) \\ &= I_\gamma\left(\bar{n} + \bar{q}_{d2} + \bar{k}_{1max}\left(\bar{k}_{1max} + 1\right)\|\chi(0)\|_2 + \bar{k}_{2max} + \bar{k}_{3max}\|\chi(0)\|_2 + \|\chi(0)\|_2\right)\end{aligned} \tag{56}$$

Suppose the inequalities (39) and (40) are hold, from (53) and (56), $h(x) \leq F_{max} = [F_{1max}, F_{2max}, F_{3max}, \tau_{\gamma max}]^T$ for all time, which means the LMPC admit recursive feasibility for all $t \geq 0$.

Theorem 0.5. *Suppose the Assumption 0.1, 0.2 and 0.3 are satisfied, then the closed-loop system under LMPC Algorithm 1 is asymptotically stable with respect to the equilibrium* $\begin{bmatrix} \xi_1 \\ \xi 2 \end{bmatrix} = \begin{bmatrix} 0 \\ 0 \end{bmatrix}$.

Proof. Since the Lyapunov function V_2 is continuously differentiable and radially unbounded, according to converse Lyapunov theorems Khalil (2002), there exist functions $\upsilon_i(\cdot), i = 1, 2, 3$ which belong to class K_∞ satisfying following inequations:

$$\upsilon_1(\|q\|) \leq V_2(q) \leq \upsilon_2(\|q\|) \tag{57}$$

$$\frac{\partial V}{\partial q} f(q, h(q)) \leq -\upsilon_3(\|q\|) \tag{58}$$

Considering that the contraction constraint and the optimal solution will be implemented for one sampling period each time, the following can be guaranteed:

$$\frac{\partial V}{\partial q} f(q, u(q)) \leq \frac{\partial V}{\partial q} f(q, h(q)) \leq -\upsilon_3(\|q\|) \tag{59}$$

By Lyapunov arguments Khalil (2002), the closed-loop system under Algorithm 1 is asymptotically stable with a guaranteed region of attraction $\mathbb{R}$

$$H = \{x \in \mathbb{R}^n | (39), (40)\} \tag{60}$$

Moreover, H can be extended by reducing the magnitude of the control gains $\bar{k}_{1max}$, $\bar{k}_{2max}$, $\bar{k}_{3max}$

Remark 5. Theoretically, according to the stability analysis, system stability is not influenced by the number of iterations in the optimization process. Therefore, the computational time for the MPC problem is not discussed here. However, it is straightforward to apply the proposed controller in the real car-driving system since the computational time of the MPC problem is effectively handled by automatic code generation technique, which is developed in several software packages such as ACADO Quirynen et al. (2015), FORCES Pro Zanelli et al. (2020), and VIATOC Kalmari et al. (2015).

Simulation results

In this section, numerical simulations for CDS are implemented to validate the advantages of the designed LMPC method. The CDS model is working under several physical constraints. Assuming that the three pistons have the same capability with the stroke length is 0.4 m, particularly the maximum force they can function is 150 N, and their length l_i $(i = 1, 2, 3)$ are limited in the range 0.4(m) to 0.8(m). In addition, the mobile panel can rotate along Oz axis with the rotation angular is in range $\left[\frac{-\pi}{2}, \frac{\pi}{2}\right]$ (rad) and the maximum rotation torque is 50 Nm.

The system parameters used for simulation include: $m_p = 15$ (kg), $m_2 = 3$ (kg), $m_{dc} = 3$ (kg), $a_z = 0.05$ (m), $a = b = c = 0.05$, (m). The reference trajectories for CDS are designed as follows:

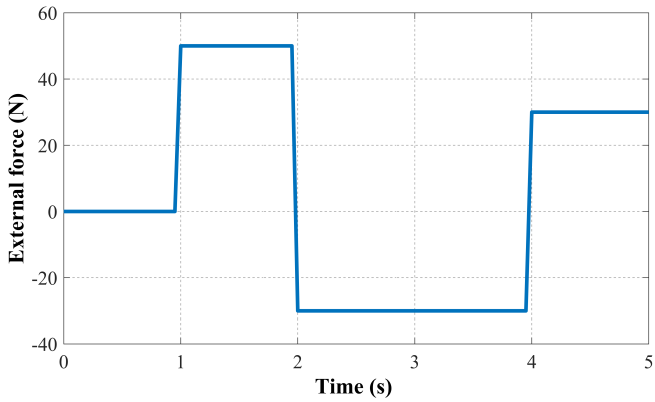

Figure 2. Vertical external disturbance

$$\begin{aligned} l_{1r} &= -0.0045t^3 + 0.034t^2 - 0.025t + 0.44 \\ l_{2r} &= -0.0008t^3 + 0.0175t^2 - 0.011t + 0.7 \\ l_{3r} &= 0.0008t^3 - 0.0125t^2 + 0.072t + 0.5 \\ \gamma_r &= 0.004t^3 - 0.0625t^2 + 0.4t \end{aligned} \tag{61}$$

with $x\left(0\right) = \left[0.55, 0.6, 0.6, 0, 0, 0, 0, 0\right]^T$ is the initial values.

The parameters for LMPC controller are chosen as follows: the sampling period $h = 0.05$ (s), the prediction horizon $T_h = 5h$, the weighting matrices $P = Q = \text{diag}\left(\left[10^5, 10^5, 10^5, 2\times10^5, 10^3, 10^3, 10^3, 1\right]\right)$, $R = \text{diag}\left(\left[1, 1, 1, 0.1\right]\right)$. To numerically solve the LMPC problems, Runge-Kutta 4th order method is employed to discretize the problem, and then the sequential quadratic programming (SPQ) method is used to handle the Karush-Kuhn-Tucker (KKT) conditions. For the fuzzy logic system, the Gaussian membership function is selected for each input, and the adaptive gain matrix is $\Gamma = \text{diag}\left(\left[500, 500, 500, 100\right]\right)$.

Two simulation scenarios are conducted which consider different conditions of external forces and uncertainties of the model to evaluate the quality of the proposed controller. The results of two simulation scenarios are illustrated as follows.

Scenario 1

The CDS model in this circumstance endures the external force in the vertical direction, which is depicted in Fig. 2.

The main advantage of the MPC controller is that it can effectively handle the hard constraints while maintaining high performance for the system. Therefore, the comparisons between the proposed LMPC controllers (LMPCF) with adaptive fuzzy BSMC (BSMCF) and original LMPC controllers (LMPC) are conducted under the impact of the external force to the CDS system.

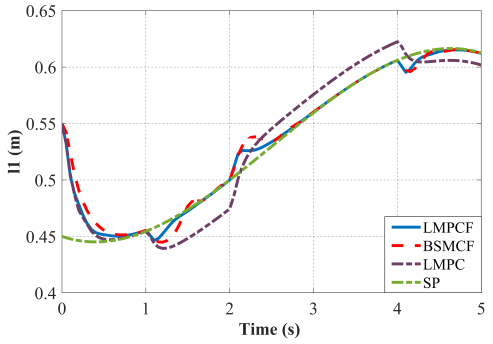

(a) Tracking trajectory of l_1

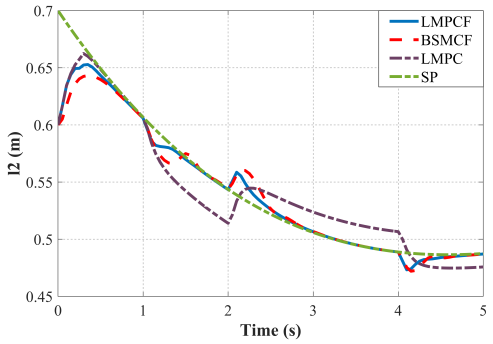

(b) Tracking trajectory of l_2

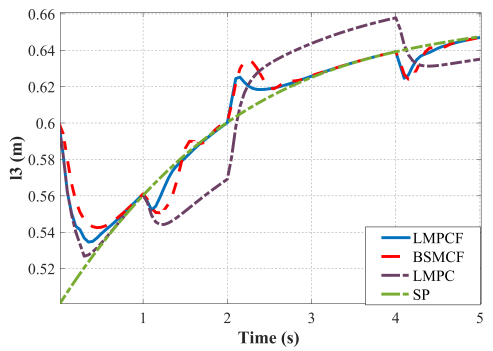

(c) Tracking trajectory of l_3

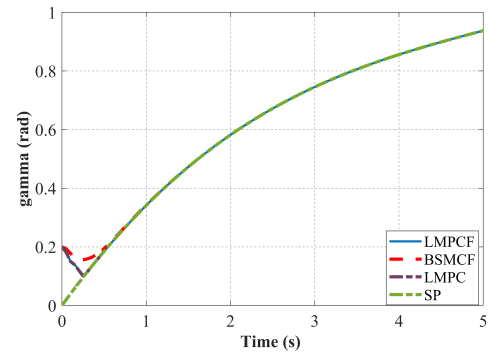

(d) Tracking trajectory of γ

Figure 3. Tracking trajectories of CDS in Scenario 1

The parameters used for LMPC are similar to the proposed controller, and the Fuzzy laws of BSMCF are similar to the Fuzzy laws of the proposed controller. The control gains for BSMCF are $K_1 = K_2 = K_3 = \text{diag}(1, 1, 1, 1)$.

The trajectory tracking results are presented in Fig. 3. The small control gain matrices K_1, K_2, K_3 are opted to ensure a large region of attraction, which means the BSMCF can satisfy system constraints. However, the performance of the LMPC controller strongly depends on the accuracy of the system model to predict future state trajectories used for optimization. Hence, the original LMPC controller cannot compensate for the model error when the external disturbance is added, leading to the worst performance. On the other hand, with the assistance of the fuzzy approximation system and adaptive law, BSMCF and LMPCF can meet the control requirement in the presence of disturbance.

To be more specific, the tracking errors of system states are depicted in Fig. 4. When the external disturbance changes its value in instant 1s, 2s, and 4s, the LMPCF and BSMCF controller quickly drive the system back to the desired positions owning to the fuzzy approximation system while the original LMPC cannot compensate for the difference of system model. The LMPCF controller converges faster

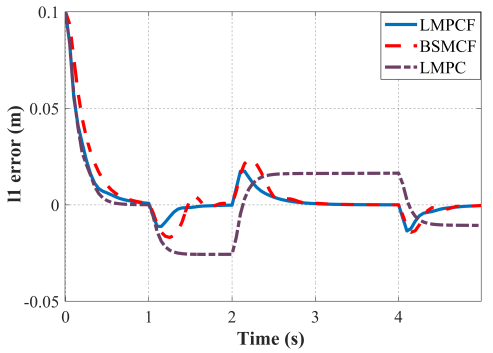

(a) Tracking error of l_1

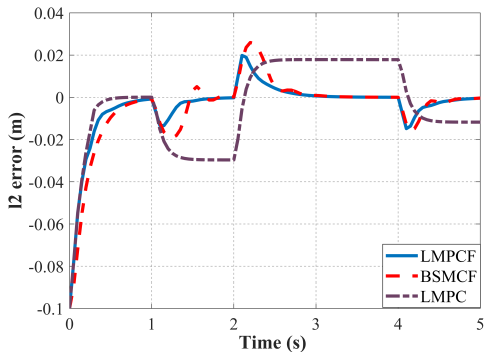

(b) Tracking error of l_2

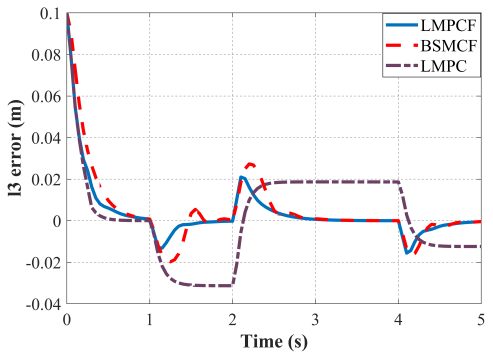

(c) Tracking error of l_3

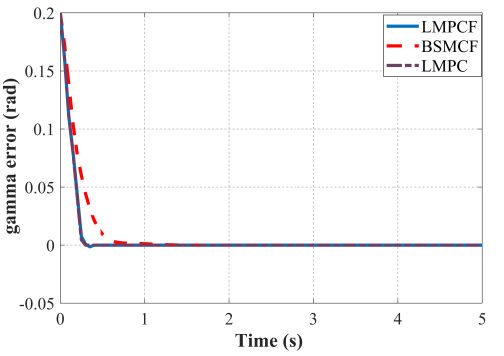

(d) Tracking error of γ

Figure 4. Tracking errors of the CDS in Scenario 1

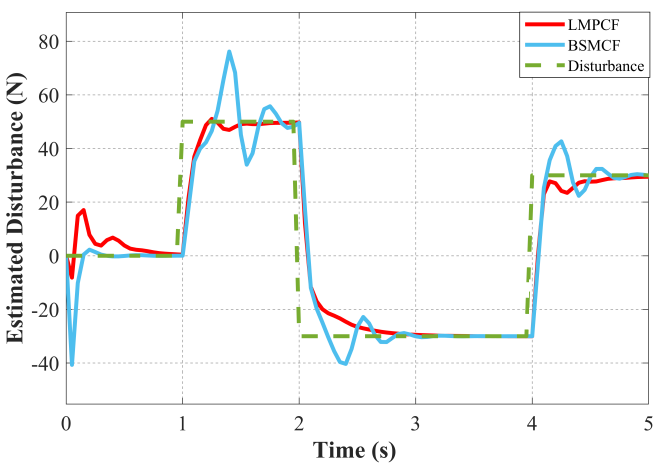

Figure 5. External disturbance estimation of LMPC and BSMCF

Table 1. Mean Square Error with external forces - Scenario 1

MSE	LMPCF	BSMCF	LMPC
l_1 (cm^2)	2.5891	3.7668	4.4864
l_2 (cm^2)	2.5444	3.6770	5.0918
l_3 (cm^2)	2.5603	3.7920	5.3287
γ (10^{-4} rad^2)	7.0689	11.163	8.2381

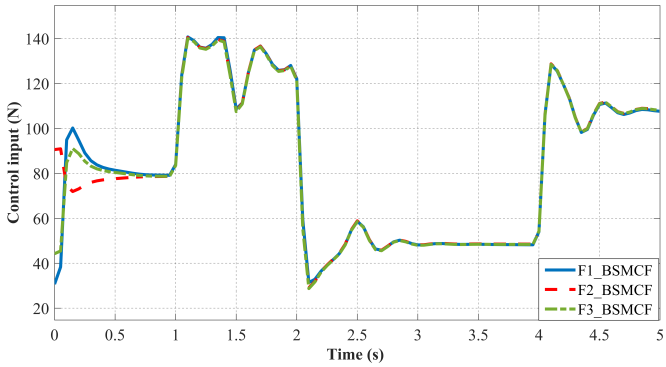

Figure 6. Control inputs of BSMCF

than two other methods, leading to its error value being also most minor, followed by BSMCF and original LMPC.

To further verify the tracking performance of the proposed controller as compared to the others, Table 1 presents the mean square error of tracking errors in Scenario 1. Initially, the values of the system's states are set to be different from those of reference trajectories (10 cm for three pistons, 11.5 degrees for rotating base); the error values then decline sharply, and after roughly 1s, the controlled outputs first reach the desired points. Afterward, the CDS is impacted by the external forces as in (2), leading to the deviation between the nominal model used to construct control signals and the actual model. Therefore, large tracking errors always exit when the LMPC controller is implemented, causing the highest MSEs in all tracking outputs. By contrast, because the external forces are estimated by the fuzzy system, the model errors are compensated in control signals generation, the MSEs of LMPCF and BSMCF controllers are reduced significantly. Especially, the MSEs of the LMPCF controller are all lower than the BSMCF controller because they are optimized with constraints to produce control signals, while these of BSMCF depend highly on the selection of control parameters K_1, K_2, and K_3.

The approximated disturbance values are presented in Fig. 5. When the disturbance changes, it takes time for the fuzzy approximation system to adapt to the current value. Therefore, there is a fluctuation in the system responses and the estimated disturbance values in the early period. The convergence speed depends on the fuzzy logic structure and the learning rate.

In addition, the control input of BSMCF and LMPCF are also shown in Fig. 6, Fig. 7. Since the LMPCF controller can explicitly handle input constraints in the optimization step, the control inputs are kept in the preconfigured range $[0, 150]$ (N). When the tracking error is high, the LMPCF controller fully utilizes

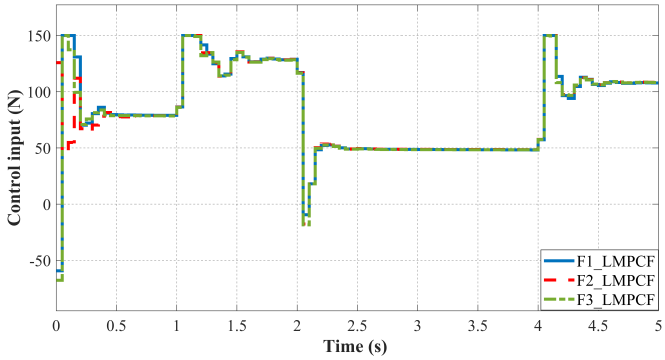

Figure 7. Control inputs of LMPCF

the piston capability to generate the fastest convergence while satisfying all constraints. Meanwhile, the control gains K_1, K_2, K_3 for BSMCF are carefully selected not to break the constraints.

Scenario 2

In this case, the robustness of the proposed controller under the effect of model uncertainties and unknown elements is presented. The comparison between the proposed method and LMPC without the assistance of the fuzzy approximation system is illustrated to show the superiority of our method. To derive the uncertainties, the system's parameters to construct the control signal are different from the values used in the dynamic model. Specifically, there exist 20% model parameter errors combined with unknown noises, which are presented as red dashed lines in Fig. 8.

To further evaluate the performance of the proposed controller, Fig. 9 shows the tracking results of the CDS.

According to Fig. 9, without the support from the fuzzy system to estimate the uncertain part, the LMPC cannot derive the system to the exact reference path because the performance of the LMPC depends heavily on the accuracy of the mathematical model. Therefore, there always exists the deviation between the reference trajectories with the control output. On the other hand, the performance of the controller is significantly improved when it is integrated with the fuzzy approximation system. In the initial period, the fuzzy system takes time to adapt to the current disturbance value. The estimated outputs of the fuzzy system are illustrated in Fig. 8. After roughly 1 second, the approximated noises follow nearly the same as the actual value, which sufficiently compensates for the uncertain part in the controller signal. Therefore, the robustness of the tracking system is considerably enhanced by the LMPCF controller. The Mean square errors (MSEs) for both comparing controllers are calculated in the Table. Clearly, the MSEs of the LMPCF are much smaller than the LMPC method. The mean square error with model uncertainties of the controllers in Scenario 2 is summarized in Table 2.

According to Table. 2, compared with the LMPC controller, the proposed controller's MSEs are smaller, which improves tracking qualities by more than 15% for piston states and by more than 5% for the rotation angle because the proposed controller is capable of estimating the model uncertainties while retaining the robustness of the LMPC controller. At the same time, the LMPC is not capable of estimating

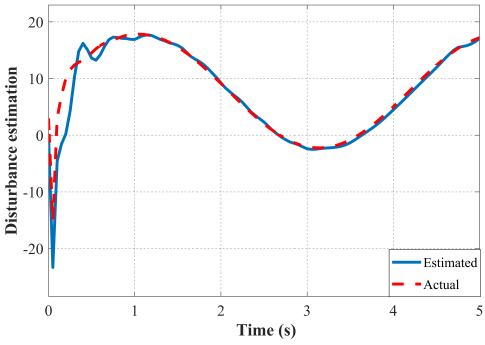

(a) The disturbance estimation of l_1

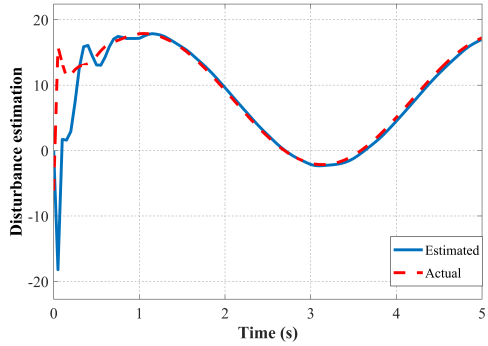

(b) The disturbance estimation of l_2

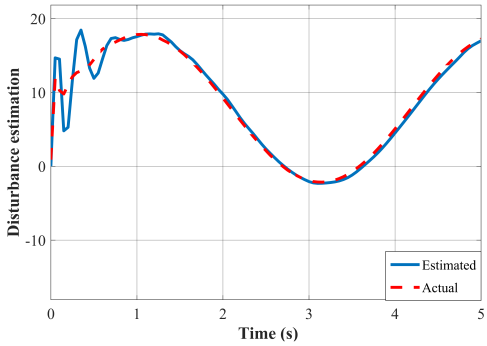

(c) The disturbance estimation of l_3

Figure 8. Disturbance estimations of the CDS in Scenario 2

Table 2. Mean Square Error with model uncertainties - Scenario 2

MSE	LMPCF	LMPC	Improvement
l_1 (cm^2)	1.8388	2.1759	15.5%
l_2 (cm^2)	2.010	2.6391	23.97%
l_3 (cm^2)	1.6694	2.1403	21.76%
γ (10^{-4} rad^2)	7.9417	7.9820	5.01%

them. By adding the contraction constraint in optimization, the MPC controller can inherit the robustness and stability of the BSMC method with respect to the white noise or low amplitude noise as presented in Kim et al. (2019), Liu et al. (2017b). Moreover, the controller is supported by the adaptive Fuzzy rule, and thus uncertain elements, as well as noises, can be approximated or compensated to improve the control quality. Hence, the proposed adaptive controller, in this case, has ability to handle with adverse factors. The simulation results show that system performance with and without consideration of these noises are nearly the same.

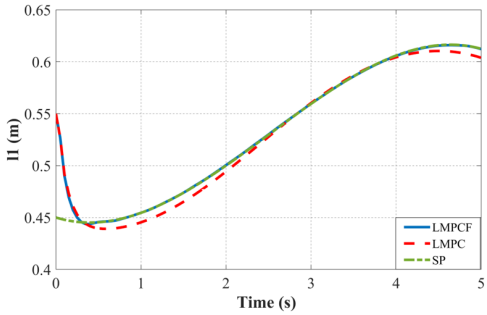

(a) Tracking trajectory of l_1

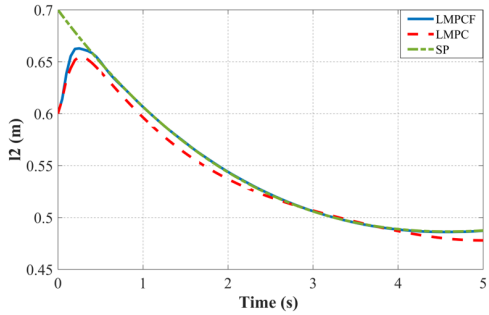

(b) Tracking trajectory of l_2

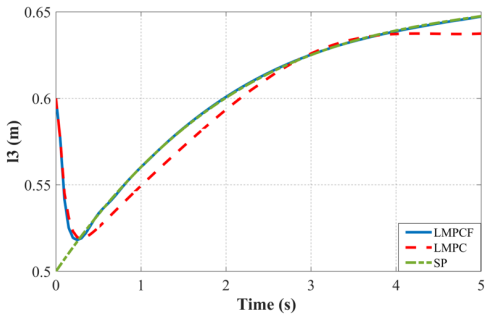

(c) Tracking trajectory of l_3

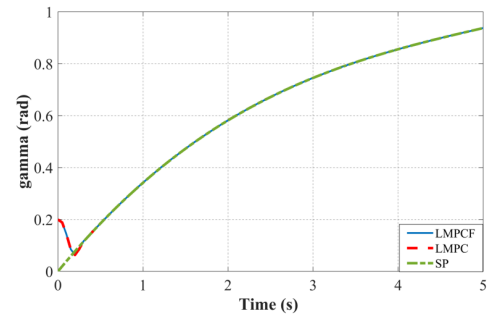

(d) Tracking trajectory of γ

Figure 9. Tracking trajectories of the CDS in Scenario 2

Conclusion

A method to cope with system constraints and uncertainties stemming from the CDS model is constructed based on the Lyapunov-based MPC integrated with the adaptive fuzzy law. By incorporating the Backstepping and SMC into the contraction condition, control performance, robustness, and stability of LMPC is significantly enhanced. Moreover, the feasibility and closed-loop stability of the proposed controller is also rigorously proven. Combined with the fuzzy technique, the system can approximate the uncertain parts along with noises, and thus the appropriate values are generated for these factors to improve the predictive model's performance. Furthermore, the simulation results show the proposed method's superiority and efficiency compared to other controllers. In the future, experiments on the real CDS model will be conducted to evaluate more accurately the performance of the proposed controller. The fuzzy approximation system can be upgraded to respond more quickly to the change of the disturbances. Besides, an observer is projected to be designed to estimate the system states which are normally difficult to measure accurately in practice.

Acknowledgement

This research is funded by the Hanoi University of Science and Technology (HUST) under project number T2021-PC-001.

Bibliography

Baigzadehnoe B, Rahmani Z, Khosravi A and Rezaie B (2017) On position/force tracking control problem of cooperative robot manipulators using adaptive fuzzy backstepping approach. *ISA transactions* 70: 432–446.

Campa R, Bernal J and Soto I (2016) Kinematic modeling and control of the hexapod parallel robot. In: *2016 American Control Conference (ACC)*. pp. 1203–1208.

Choubey C and Ohri J (2022) Tuning of lqr-pid controller to control parallel manipulator. *Neural Computing and Applications* 34(4): 3283–3297.

Christofides PD, Liu J and De La Pena DM (2011) *Networked and distributed predictive control: Methods and nonlinear process network applications*. Springer Science & Business Media.

Dindorf R and Wos P (2019) Design of a hydraulically actuated 3-dof translational parallel manipulator. *AIP Conference Proceedings* 2077(1): 020015.

Godbole H, Caverly R and Forbes J (2019) Dynamic modeling and adaptive control of a single degree-of-freedom flexible cable-driven parallel robot. *Journal of Dynamic Systems, Measurement and Control, Transactions of the ASME* 141(10). Funding Information: Dr. J. R. Forbes would like to thank Dr. C. J. Damaren for discussing with him how to best find the parameter μ and the insight to use μ-plots. The authors greatly appreciate the funding provided by the NSERC Discovery Grant number RGPIN-2016-04692. Publisher Copyright: Copyright © 2019 by ASME.

Gouttefarde M, Collard JF, Riehl N and Baradat C (2015) Geometry selection of a redundantly actuated cable-suspended parallel robot. *IEEE Transactions on Robotics* 31(2): 501–510.

Han J, Hu Y and Dian S (2018) The state-of-the-art of model predictive control in recent years. *IOP Conference Series: Materials Science and Engineering* 428: 012035.

Hao R, Wang J, Zhao J and Wang S (2016) Observer-based robust control of 6-dof parallel electrical manipulator with fast friction estimation. *IEEE Transactions on Automation Science and Engineering* 13(3): 1399–1408.

Hoang N and Vuong V (2018) Sliding mode control for parallel robots driven by electric motors in task space. *Journal of Computer Science and Cybernetics* 33: 325–337.

Inel F, Medjbouri A and Carbone G (2021) A non-linear continuous-time generalized predictive control for a planar cable-driven parallel robot. *Actuators* 10(5).

Jamshidifar H, Fidan B, Gungor G and Khajepour A (2015) Adaptive vibration control of a flexible cable driven parallel robot. *IFAC-PapersOnLine* 48(3): 1302–1307. 15th IFAC Symposium onInformation Control Problems inManufacturing.

Ji H, Shang W and Cong S (2020) Adaptive control of a spatial 3-degree-of-freedom cable-driven parallel robot with kinematic and dynamic uncertainties. In: *2020 5th International Conference on Advanced Robotics and Mechatronics (ICARM)*. pp. 142–147.

Jin Y, Chanal H and Paccot F (2015) *Parallel Robots*. London: Springer London. ISBN 978-1-4471-4670-4, pp. 2091–2127.

Kalmari J, Backman J and Visala A (2015) A toolkit for nonlinear model predictive control using gradient projection and code generation. *Control Engineering Practice* 39: 56–66.

Khalifa A, Fanni M, Mohamed AM and Miyashita T (2018) Development of a new 3-dof parallel manipulator for minimally invasive surgery. *The International Journal of Medical Robotics and Computer Assisted Surgery* 14(3): e1901. E1901 rcs.1901.

Khalil HK (2002) *Nonlinear systems; 3rd ed.* Upper Saddle River, NJ: Prentice-Hall. The book can be consulted by contacting: PH-AID: Wallet, Lionel.

Kiani A and Mashhadi S (2017) Lyapunov-based adaptive control of a cable-driven parallel robot. *International Journal of Advanced Mechatronic Systems* 7: 193.

Kim Y, Oh TH, Park T and Lee JM (2019) Backstepping control integrated with lyapunov-based model predictive control. *Journal of Process Control* 73: 137–146.

Li J, Sun J, Liu L and Xu J (2021) Model predictive control for the tracking of autonomous mobile robot combined with a local path planning. *Measurement and Control* : 00202940211043070.

Liu C, Gao J and Xu D (2017a) Lyapunov-based model predictive control for tracking of nonholonomic mobile robots under input constraints. *International Journal of Control, Automation and Systems* 15.

Liu C, Gao J and Xu D (2017b) Lyapunov-based model predictive control for tracking of nonholonomic mobile robots under input constraints. *International Journal of Control, Automation and Systems* 15(5): 2313–2319.

Lu X, Zhao Y and Liu M (2018) Self-learning interval type-2 fuzzy neural network controllers for trajectory control of a delta parallel robot. *Neurocomputing* 283: 107–119.

Lv W, Tao L and Ji Z (2017) Sliding mode control of cable-driven redundancy parallel robot with 6 dof based on cable-length sensor feedback. *Mathematical Problems in Engineering* 2017: 1928673.

Manh CN, Manh TN, Kim DHT, Van QN and Nguyen TL (2021) An adaptive neural network-based controller for car driving simulators. *International Journal of Control* 0(0): 1–12.

Oumer AM and Hunde AN (2015) Higher order sliding mode control of a parallel robot. In: *AFRICON 2015*. pp. 1–5.

Qinyang G, Guang-lin S, Chang-yu H, Dongmei W and Jie H (2017) Adaptive robust dynamic surface control of electro-hydraulic system with unknown nonlinear disturbance.

Quan DM, Tuan DA, My TC and Hung LQ (2020) Building the control signal model for design of 3dof motion platform of marine simulation system 1679: 022012.

Quirynen R, Vukov M, Zanon M and Diehl M (2015) Autogenerating microsecond solvers for nonlinear mpc: a tutorial using acado integrators. *Optimal Control Applications and Methods* 36(5): 685–704.

Ramírez-Neria M, Sira-Ramírez H, Luviano-Juárez A and Rodrguez-Ángeles A (2015) Active disturbance rejection control applied to a delta parallel robot in trajectory tracking tasks. *Asian Journal of Control* 17(2): 636–647.

Rastegarpanah A, Saadat M, Borboni A and Stolkin R (2016) Application of a parallel robot in lower limb rehabilitation: A brief capability study. In: *2016 International Conference on Robotics and Automation for Humanitarian Applications (RAHA)*. pp. 1–6.

Salas FG, Orrante-Sakanassi J, del Toro RJ and Parada RP (2019) A stable proportional–proportional integral tracking controller with self-organizing fuzzy-tuned gains for parallel robots. *International Journal of Advanced Robotic Systems* 16(1): 1729881418819956.

Santos JC, Chemori A and Gouttefarde M (2019) Model predictive control of large-dimension cable-driven parallel robots. In: Pott A and Bruckmann T (eds.) *Cable-Driven Parallel Robots*. Cham: Springer International Publishing. ISBN 978-3-030-20751-9, pp. 221–232.

Song Y and Huh K (2021) Driving and steering collision avoidance system of autonomous vehicle with model predictive control based on non-convex optimization. *Advances in Mechanical Engineering* 13(6):

16878140211027669.

Thi KDH, Nguyen MC, Vo HT, Tran VM, Nguyen DD and Bui AD (2019) Trajectory tracking control for four-wheeled omnidirectional mobile robot using backstepping technique aggregated with sliding mode control. In: *2019 First International Symposium on Instrumentation, Control, Artificial Intelligence, and Robotics (ICA-SYMP)*. pp. 131–134.

Thomas MJ, George S, Sreedharan D, Joy M and Sudheer A (2022) Dynamic modeling, system identification and comparative study of various control strategies for a spatial parallel manipulator. *Proceedings of the Institution of Mechanical Engineers, Part I: Journal of Systems and Control Engineering* 236(2): 270–293.

Tian Z (2021) Networked control system time-delay compensation based on pi-based dynamic matrix control. *at - Automatisierungstechnik* 69(1): 41–51.

Tian Z and Wang Y (2022) Predictive control compensation for networked control system with time-delay. *Proceedings of the Institution of Mechanical Engineers, Part I: Journal of Systems and Control Engineering* 236(1): 107–124.

Tien KN, Kim DHT, Manh TN, Manh CN, Van Bach NP and Quang HD (2019) Adaptive dynamic surface control for car driving simulator based on artificial neural network. In: *2019 International Conference on Mechatronics, Robotics and Systems Engineering (MoRSE)*. pp. 192–197.

Truong TN, Vo AT and Kang HJ (2021) A backstepping global fast terminal sliding mode control for trajectory tracking control of industrial robotic manipulators. *IEEE Access* 9: 31921–31931.

Wang Y, Lin Q, Zhou L, Shi X and Wang L (2020a) Backstepping sliding mode robust control for a wire-driven parallel robot based on a nonlinear disturbance observer. *Mathematical Problems in Engineering* 2020: 1–17.

Wang Y, Lin Q, Zhou L, Shi X and Wang L (2020b) Backstepping sliding mode robust control for a wire-driven parallel robot based on a nonlinear disturbance observer. *Mathematical Problems in Engineering* 2020.

Wen S, Chen J, Qin G, Zhu Q and Wang H (2018) An improved fuzzy model predictive control algorithm based on the force / position control structure of the five-degree of freedom redundant actuation parallel robot. *International Journal of Advanced Robotic Systems* 15(5): 1729881418804979.

Wu TS, Karkoub M, Yu WS, Chen CT, Her MG and Wu KW (2016) Anti-sway tracking control of tower cranes with delayed uncertainty using a robust adaptive fuzzy control. Elsevier, pp. 118–137.

Xu J, Wang Q and Lin Q (2018) Parallel robot with fuzzy neural network sliding mode control. *Advances in Mechanical Engineering* 10(10): 1687814018801261.

Yu J, Shi P and Zhao L (2018) Finite-time command filtered backstepping control for a class of nonlinear systems. *Automatica* 92: 173–180.

Zanelli A, Domahidi A, Jerez J and Morari M (2020) Forces nlp: an efficient implementation of interior-point methods for multistage nonlinear nonconvex programs. *International Journal of Control* 93(1): 13–29.

Zhang H, Fang H, Zhang D, Luo X and Zou Q (2020a) Adaptive fuzzy sliding mode control for a 3-dof parallel manipulator with parameters uncertainties. *Complexity* 2020: 2565316.

Zhang H, Fang H, Zhang D, Luo X and Zou Q (2020b) Adaptive fuzzy sliding mode control for a 3-dof parallel manipulator with parameters uncertainties. *Complexity* 2020.

Zhengsheng C, Xuesong W and Yuhu C (2021) Adaptive super-twisting algorithm-based fractional-order sliding mode control of redundantly actuated cable driving parallel robot with uncertainty and disturbance estimation. *IET Control Theory & Applications* 15(18): 2243–2257.